Arabidopsis Novel Glycine-Rich Plasma Membrane PSS1 Protein Enhances Disease Resistance in Transgenic Soybean Plants[1][OPEN]

Bing Wang,[2] Rishi Sumit,[2] Binod B. Sahu, Micheline N. Ngaki, Subodh K. Srivastava, Yang Yang, Sivakumar Swaminathan, and Madan K. Bhattacharyya[3]

Department of Agronomy, Iowa State University, Ames, Iowa 50011

ORCID IDs: 0000-0002-2151-0654 (B.B.S.); 0000-0002-8765-2372 (M.N.N.); 0000-0002-5639-9706 (M.K.B.).

Nonhost resistance is defined as the immunity of a plant species to all nonadapted pathogen species. Arabidopsis (*Arabidopsis thaliana*) ecotype Columbia-0 is nonhost to the oomycete plant pathogen *Phytophthora sojae* and the fungal plant pathogen *Fusarium virguliforme* that are pathogenic to soybean (*Glycine max*). Previously, we reported generating the *pss1* mutation in the *pen1-1* genetic background as well as genetic mapping and characterization of the Arabidopsis nonhost resistance *Phytophthora sojae*-susceptible gene locus, *PSS1*. In this study, we identified six candidate *PSS1* genes by comparing single-nucleotide polymorphisms of (1) the bulked DNA sample of seven $F_{2:3}$ families homozygous for the *pss1* allele and (2) the *pen1-1* mutant with Columbia-0. Analyses of T-DNA insertion mutants for each of these candidate *PSS1* genes identified the *At3g59640* gene encoding a glycine-rich protein as the putative *PSS1* gene. Later, complementation analysis confirmed the identity of *At3g59640* as the *PSS1* gene. *PSS1* is induced following *P. sojae* infection as well as expressed in an organ-specific manner. Coexpression analysis of the available transcriptomic data followed by reverse transcriptase-polymerase chain reaction suggested that *PSS1* is coregulated with *ATG8a* (*At4g21980*), a core gene in autophagy. PSS1 contains a predicted single membrane-spanning domain. Subcellular localization study indicated that it is an integral plasma membrane protein. Sequence analysis suggested that soybean is unlikely to contain a PSS1-like defense function. Following the introduction of *PSS1* into the soybean cultivar Williams 82, the transgenic plants exhibited enhanced resistance to *F. virguliforme*, the pathogen that causes sudden death syndrome.

Nonhost resistance is defined as immunity of an entire plant species against all races or isolates of a nonadapted pathogen species. Examples include fungi and oomycete pathogens that fail to penetrate and propagate in the nonhost plants (Heath, 2000; Mysore and Ryu, 2004; Lipka et al., 2005; Senthil-Kumar and Mysore, 2013; Hadwiger, 2015; Lee et al., 2016). It is widely considered that nonhost resistance mechanisms are multilayered and are often elicited by pathogen-associated molecular patterns (PAMPs; Jones and Dangl, 2006). Upon failure of the pathogens to invade a nonhost due to the activation of basal host resistance triggered by PAMPs (PAMP-triggered immunity), effectors are secreted by the phytopathogens to derive nutrition and interfere with the host defense physiology, leading to the development of susceptibility known as effector-triggered susceptibility. Host plants then express cognate *R* genes encoding receptors that recognize one or more of these effectors and trigger immunity (effector-triggered immunity), which is manifested commonly as a hypersensitive reaction or programmed cell death (Jones and Dangl, 2006).

A mutant study identified *PENETRATION DEFICIENT1* (*PEN1*), *PEN2*, and *PEN3* genes that confer nonhost immunity of the Arabidopsis (*Arabidopsis thaliana*) ecotype Columbia-0 (Col-0) against the barley (*Hordeum vulgare*) powdery mildew pathogen *Blumeria graminis* f. sp. *hordei* (Collins et al., 2003; Lipka et al., 2005; Stein et al., 2006). Study of the three *PEN* genes revealed two parallel nonhost resistance mechanisms that suppress the penetration of *B. graminis* f. sp. *hordei*. One mechanism, regulated by PEN1, entails vesicle-mediated secretion of free radicals such as hydrogen peroxide to invasion sites. In the other mechanism, PEN2 and PEN3 regulate the transport of antimicrobial glucosinolates and Trp-derived secondary metabolites to infection sites (Clay et al., 2009; Schulze-Lefert and Panstruga, 2011). Other genes, such as *Enhanced Disease Susceptibility1*, *Phytoalexin-Deficient4*,

[1] This work was supported by USDA NIFA (grant no. 2013-68004-20374), the Iowa Soybean Association, and the Consortium of Plant Biotechnology Research.

[2] These authors contributed equally to the article.

[3] Address correspondence to mbhattac@iastate.edu.

The author responsible for distribution of materials integral to the findings presented in this article in accordance with the policy described in the Instructions for Authors (www.plantphysiol.org) is: Madan K. Bhattacharyya (mbhattac@iastate.edu).

M.K.B. conceived and supervised the project; S.K.S. conducted the SHORE analysis; R.S. and B.B.S. cloned the *PSS1* gene; R.S., B.B.S., and M.N.N. performed the construction of binary vectors for soybean transformation and harvested R1 seeds; B.W. investigated the gene function; B.W., B.B.S., R.S., M.N.N., S.S., and Y.Y. evaluated the transgenic soybean plants; B.W., M.N.N., and R.S. analyzed the data; B.W. and R.S. wrote the first draft, and M.K.B completed writing the article.

[OPEN] Articles can be viewed without a subscription.

www.plantphysiol.org/cgi/doi/10.1104/pp.16.01982

Senescence-Associated Gene101, *Mildew Resistance Locus O2*, the UDP-glucosyltransferase *UGT84A2/BRT1*, and the calcium sensor *CaM7*, were identified to be involved in Arabidopsis nonhost resistance (Lipka et al., 2005; Stein et al., 2006, Nakao et al., 2011; Langenbach et al., 2013; Campe et al., 2016). In addition to these nonhost resistance genes, spatial and temporal changes in the production of stress hormones play major roles in nonhost immunity. For example, the involvement of salicylic acid and jasmonic acid in the expression of nonhost defense in Arabidopsis against nonadapted fungal isolates has been reported (Mellersh and Heath, 2003).

Gly-rich proteins (GRPs) belong to a protein superfamily that is characterized by the presence of a Gly-rich domain arranged in (Gly)n-X repeats. The expression of genes encoding GRPs is tissue specific, and they are often developmentally regulated or modulated by biotic and abiotic factors (Mangeon et al., 2010). GRPs are involved in a variety of functions in plants, including cell wall structure, plant defense, pollen hydration, signal transduction, osmotic stress, cold stress, flowering time control, development, and cell elongation (Mousavi and Hotta, 2005; Mangeon et al., 2010). GRPs take part in plant defense responses by maintaining cell wall components and callose deposition (Ueki and Citovsky, 2002; Lin and Chen, 2014), modulating PR-1 expression (Park et al., 2001), and displaying antimicrobial activity to inhibit the growth of microbes (Park et al., 2000; Egorov et al., 2005; Tavares et al., 2012). Aside from the Gly-rich domain, some GRPs carry RNA-binding domains. Arabidopsis AtGRP7 is a Gly-rich RNA-binding protein that regulates callose deposition in the PAMP flg22-induced FLS2-mediated immunity (Fu et al., 2007). *AtGRDP2* encodes a short Gly-rich domain protein containing a DUF1399 domain and a putative RNA recognition motif. Overexpression of *AtGRDP2* resulted in higher tolerance of Arabidopsis to salinity stress (Ortega-Amaro et al., 2015).

Arabidopsis is a model plant with T-DNA mutants available for most of its genes, making it suitable for studying nonhost resistance mechanisms (Alonso et al., 2003; Rhee et al., 2003). We previously reported the identification of 30 *Phytophthora sojae*-susceptible mutants named *pss1* through *pss30* from screening of over 3,500 ethylmethane sulfonate (EMS)-induced M2 families. The *pss1* mutant was shown to be susceptible also to *Fusarium virguliforme* (Sumit et al., 2012). *PSS1* was genetically mapped to chromosome 3 by bulked segregant analysis (Sumit et al., 2012). In this study, we applied SHORE mapping to identify six candidate *PSS1* genes (Schneeberger et al., 2009). Analyses of T-DNA insertion mutants of the candidate *PSS1* genes led to the identification of the *At3g59640* gene that complemented EMS-induced *pss1* and two T-DNA insertion-induced *pss1* mutants. We showed that PSS1 localizes to the plasma membrane. Furthermore, we identified that, upon stable transformation, *PSS1* enhances resistance to the fungal pathogen *F. virguliforme* in transgenic soybean (*Glycine max*) plants.

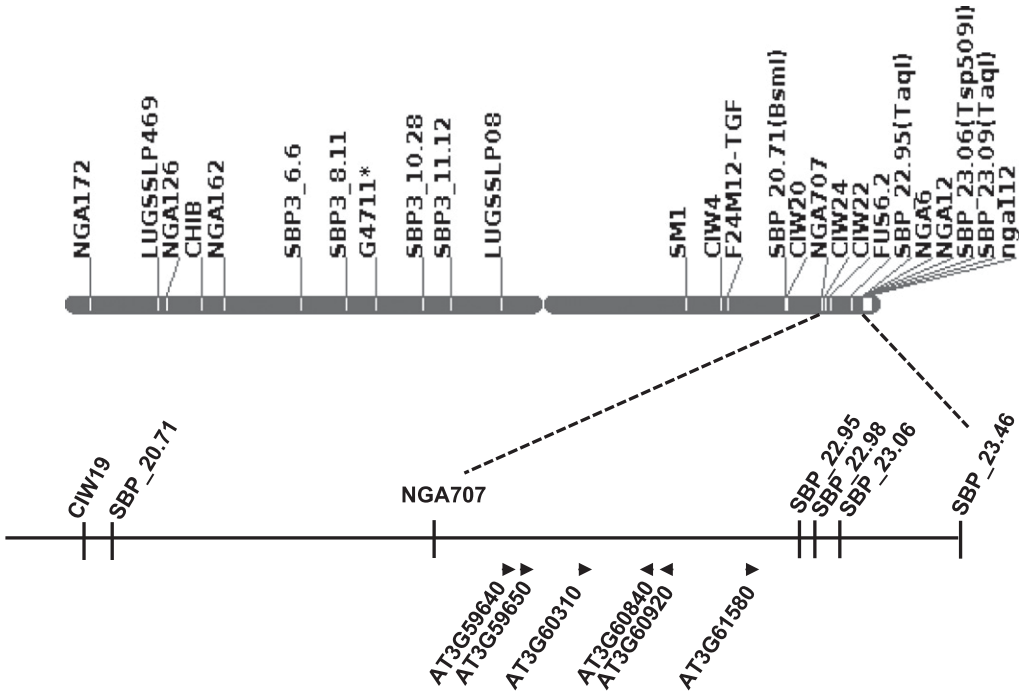

Figure 1. Candidate nonhost resistance *PSS1* genes. The six putative nonhost-resistant genes are shown in a 1.2-Mb genomic region flanked by NGA707 and SBP_22.95 markers mapped to chromosome 3. The arrowheads indicate the orientations of six candidate *PSS1* genes on the Arabidopsis Col-0 genome sequence.

Table I. *Six candidate PSS1 genes carrying nonsynonymous mutations between the NGA707 and SBP_22.95 markers mapped to Arabidopsis chromosome 3*

Single-Nucleotide Polymorphism	Locus	Annotation	Base Change	Substitution
22029832	AT3G59640	Gly-rich protein	G-A	Gly/Asp
22033274	AT3G59650	Mitochondrial protein	G-A	Gly/Asp
22290347	AT3G60310	Unknown protein	G-A	Ala/Thr
22477739	AT3G60840	Microtubule-associated protein	G-A	Pro/Leu
22504152	AT3G60920	BEACH domain proteins	G-A	Ala/Asp
22786292	AT3G61580	Sphingoid LCB desaturase	G-A	Asp/Asn

RESULTS

The Nonhost Resistance *PSS1* Gene Encodes a GRP

PSS1 was mapped to a 2.75-Mb genomic region between markers SBP_20.71 and SBP_23.46 on chromosome 3 (Sumit et al., 2012; Fig. 1). Comparison of the sequence of the *PSS1* region in a bulked DNA sample generated from seven $F_{2:3}$ homozygous families for the *pss1* allele with that of the Col-0 genome sequence revealed 30 point mutations or single-nucleotide polymorphisms. Nine of these mutations were nonsynonymous. The *pss1* mutant was generated in the

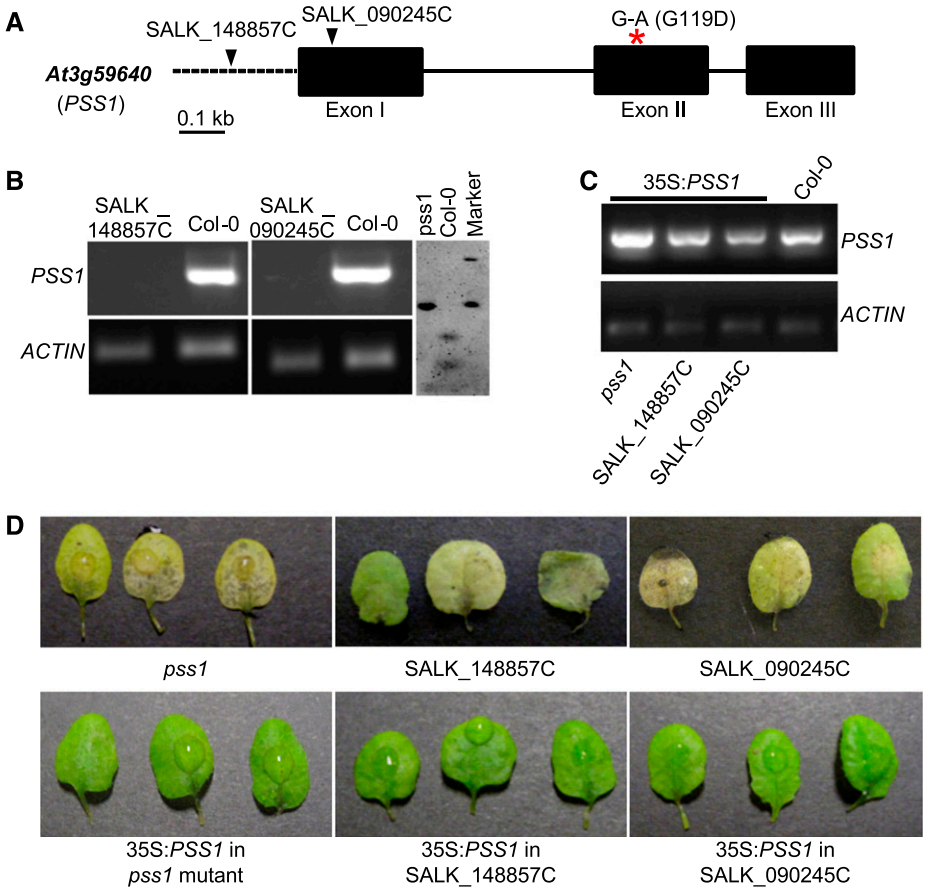

Figure 2. Identification of *PSS1* through mutant and complementation analyses. A, Analyses of T-DNA mutants in the *At3g59640* gene. The locations of the T-DNA insertions in the *At3g59640* gene between the two *P. sojae*-susceptible T-DNA mutants, SALK_090245C and 148857C, are shown by arrowheads. The red asterisk shows the nonsynonymous transition G-to-A mutation in exon II, which results in the substitution of Gly (G) to Asp (D) at position 119 in the pss1 mutant protein. Black boxes represent three exons, and the lines connecting exons represent introns. The promoter is shown with a dashed line. B, Molecular analyses of *pss1* mutants. RT-PCR confirms the absence of *PSS1* transcripts in two T-DNA mutants shown at left. The EMS-induced *pss1* mutant is confirmed by *Aci*I enzyme digestion of the PCR products of genomic DNA from *pss1* and Col-0. Note that the transition mutation led to loss of the restriction site in the *pss1* mutant. C, Molecular analyses of the *PSS1* cDNA-transformed *pss1* mutants. Electrophoresis is shown for PCR-amplified *PSS1* gene sequences from the EMS-induced *pss1* mutant and the SALK_148857C and SALK_090245C T-DNA mutants transformed with the 35S:*PSS1* cDNA gene. D, *PSS1* complemented the *pss1* mutants. Phenotypes of the *pss1* and two T-DNA insertion mutants in the *At3g59640* gene and their respective complemented transgenic plants 3 d following *P. sojae* infection are shown.

Col-0 *pen1-1* mutant background (Sumit et al., 2012). Three of the nine nonsynonymous mutations are common to both *pen1-1* and *pss1* mutants and were not considered for further study. The six candidate *PSS1* genes, each carrying one *pss1*-specific nonsynonymous mutation, are presented in Figure 1 and Table I.

To identify the candidate *PSS1* gene, 25 T-DNA knockout mutants for the six candidate *PSS1* genes (Supplemental Table S1) were evaluated for response to *P. sojae* infection. Of the 25 lines tested, only two T-DNA lines, SALK_090245C and SALK_148857C, showed susceptibility to *P. sojae*. SALK_090245C and SALK_148857C contain T-DNA insertions in exon 1 and the promoter, respectively, of the *At3g59640* gene (Fig. 2A). Reverse transcriptase (RT)-PCR failed to detect *At3g59640* transcripts in either T-DNA insertion line (Fig. 2B). The *pss1* and two T-DNA mutants were transformed with the *At3g59640* cDNA fused to the cauliflower mosaic virus (CaMV) 35S promoter. PCR amplification confirmed the stable integration of the *At3g59640* transgene in the *pss1*, SALK_148857C, and SALK_090245C mutants transformed with the 35S:*At3g59640* cDNA fusion gene (Fig. 2C). The 35S:*At3g59640*-transformed *pss1* and T-DNA insertion *pss1* mutants expressed immunity to *P. sojae*, suggesting that *At3g59640* complemented the lost immunity function of the *pss1* mutants (Fig. 2D; Supplemental Fig. S1). Therefore, we concluded that *At3g59640* is the *PSS1* gene.

PSS1 encodes a GRP with unknown function. Apart from the Gly-rich motif (amino acids 119–154; Fig. 3A), PSS1 also contains a predicted transmembrane motif (amino acids 158–175; Fig. 3B). In the EMS-induced *pss1* mutant allele, a Gly residue is substituted with an Asp residue at position 119. This mutation is located within the conserved Gly-rich domain (Fig. 3A). We hypothesized that the change in this conserved residue led to a change in the protein structure of PSS1 and a loss of the immunity function. To investigate this, we predicted structures of PSS1 and its mutant proteins using the I-TASSER program (Zhang, 2008). Pairwise structure alignment suggested that the pss1 mutant protein possesses low structural similarity to PSS1 (TM-align score = 0.26, less than the threshold of 0.5; Supplemental Fig. S2; Zhang and Skolnick, 2005).

Based on the arrangement of Gly-rich units, PSS1 is classified as a member of the class VII GRPs that carry a mixed pattern of Gly-rich repeats (Mangeon et al., 2010). A sequence similarity search with BLASTP identified 93 plant proteins with amino acid identity greater than 33% to PSS1 with $E < 1e\text{-}25$. None of the 93 PSS1 homologs have been characterized. A few of them have been predicated to be Major Histocompatibility Complex Class II Regulatory Factor (XP_013615797; *Brassica oleracea*), Autophagy-Related Protein3 (JAT40787; *Anthurium amnicola*), and Nuclear Envelope Protein (NP_850396; Arabidopsis). The constructed neighbor-joining phylogenetic tree revealed that PSS1 clustered in a subclade with 10 homologs of the Brassicaceae family (Fig. 4). Alignment of these 10 PSS1 homologs and PSS1 revealed that the Gly-rich motifs and transmembrane domains were highly conserved among these GRPs (Supplemental Fig. S3). The soybean PSS1 homologs were placed in a distinct subclade (Fig. 4). Further study is warranted to determine if any of the genes is orthologous to PSS1 and governs any defense function.

PSS1 Is Induced in Response to *P. sojae* Infection

PSS1 has shown no homology to any protein with known function (searched on August 16, 2017). *pss1* and knockout T-DNA insertion mutants did not show any discernible defects in general growth and root development (data not shown). To address the biological function of *PSS1*, quantitative reverse transcriptase (qRT)-PCR was performed. The *PSS1* expression pattern also was examined by searching the Arabidopsis eFP Browser (http://bar.utoronto.ca/), which contains an extensive collection of gene expression microarray data (Winter et al., 2007). *PSS1* is induced following infection not only with *P. sojae* (Fig. 5A) but also at least 1.5-fold following infection with several pathogens, including *Golovinomyces orontii*, *Hyaloperonospora arabidopsidis*, and *Pseudomonas syringe*, as well as in response to treatments with various elicitors, including Hrpz and

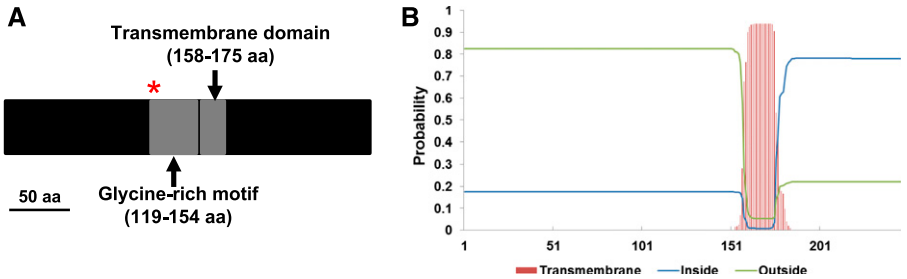

Figure 3. *PSS1* encodes a GRP containing a putative Gly-rich motif and a transmembrane domain. A, Schematic diagram of the PSS1 protein. The red asterisk indicates the substitution of Gly-119 with the Asp residue in *pss1* mutant, and two gray boxes represent a Gly-rich motif (amino acid residues [aa] 119–154) and a transmembrane domain (amino acid residues 158–175). B, Predicted transmembrane helix between amino acid residues 158 and 175 of PSS1 (greater than 90% certainty).

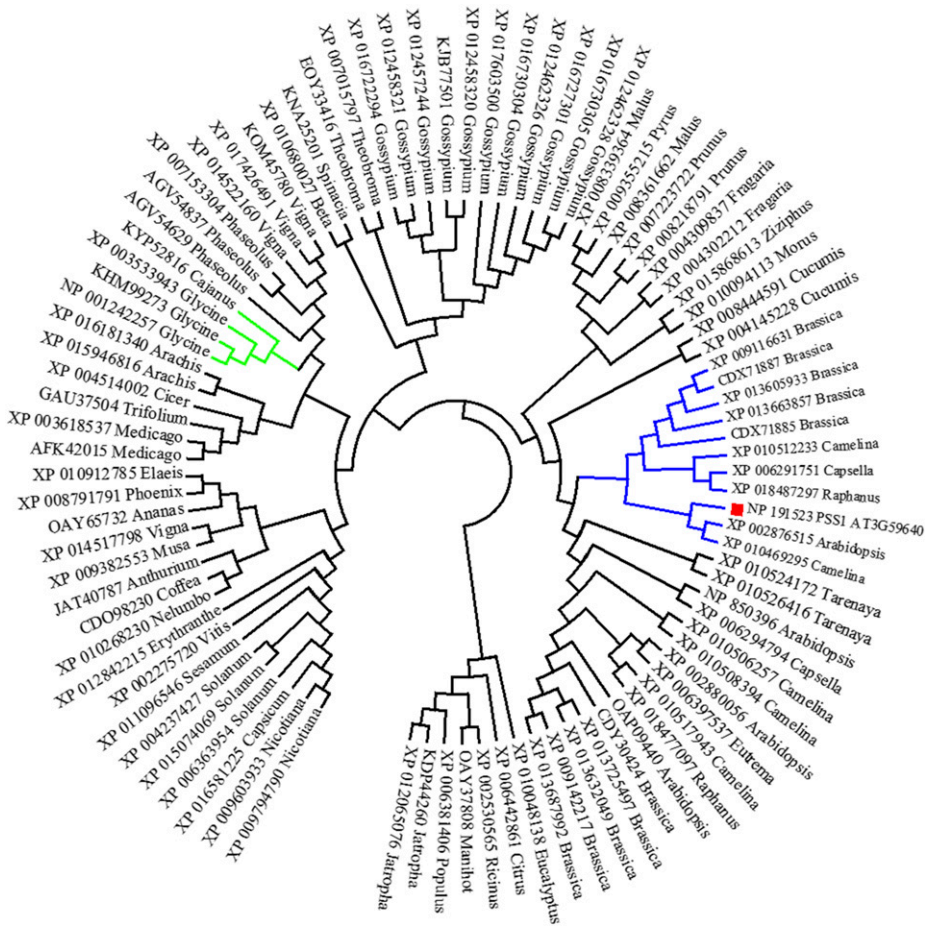

Figure 4. Phylogenetic tree of the PSS1 homologs. Ninety-three PSS1 homologs were used to construct the phylogenetic tree. PSS1 is denoted with the red rectangle. The subclade containing PSS1 is shown in blue, whereas the subclade with soybean PSS1 homologs is presented in green. The percentage identity between PSS1 and soybean homologs is 38% or less.

flg22 (Supplemental Table S2). *PSS1* expression is highest in siliques (Fig. 5B).

Coexpressed genes with the same transcriptional regulatory pathway could be functionally related, or they could be members of the same biochemical or regulatory pathway or protein complexes. We conducted initial coexpression analysis using a data set from a microarray platform available at ATTED-II (http://atted.jp/; Obayashi et al., 2007). Gene Ontology and Kyoto Encyclopedia of Genes and Genomes (Kanehisa and Goto, 2000) enrichment analyses suggested that the coexpression network is related to three biological functions: autophagy, *para*-aminobenzoic acid metabolic process, and nuclear mRNA splicing via spliceosome (Supplemental Fig. S4; Kerrien et al., 2007). To avoid any biases resulting from the use of a single data set, coexpression analysis was conducted also for the mRNA sequencing (mRNAseq) data set available at Genevestigator (Hruz et al., 2008). Gene Ontology enrichment analysis of the top 25 coexpressed genes suggested that the genes were putatively involved in three biological processes: (1) autophagy, (2) protein targeting to the vacuole, and (3) vesicle-mediated transport (Fig. 5C). Utilization of different gene expression data sets is expected to yield reliable information (Ballouz et al., 2015). To validate the outcomes of the coexpression analyses (Fig. 5C; Supplemental Fig. S4), we conducted semiquantitative RT-PCR of eight genes (Supplemental Table S3) selected from both mRNAseq and microarray data sets and observed that the autophagy-related gene *ATG8a* (*At4g21980*) is induced upon *P. sojae* infection (Supplemental Table S3). *ATG8a* is the core gene in autophagy (Yoshimoto et al., 2004). These results indicate a possible connection of PSS1 to an autophagy-related defense mechanism (Liu et al., 2005).

PSS1 Was Localized to the Plasma Membrane

Investigation of PSS1 using a transmembrane prediction program (http://cbs.dtu.dk/services/TMHMM/) revealed that it contains a single transmembrane domain between residues 158 and 175 (Fig. 3B). The Cell eFP browser (http://bar.utoronto.ca/cell_efp/cgi-bin/cell_efp.cgi; Winter et al., 2007) predicated that PSS1 could reside in nuclei, mitochondria, chloroplast, and plasma membrane. SignalP 4.0, however, did not identify any secretory signal peptides in PSS1. We expressed enhanced GFP (eGFP)-fused PSS1 (GFP-PSS1 and PSS1-GFP) transiently in *Nicotiana benthamiana* (Fig. 6).

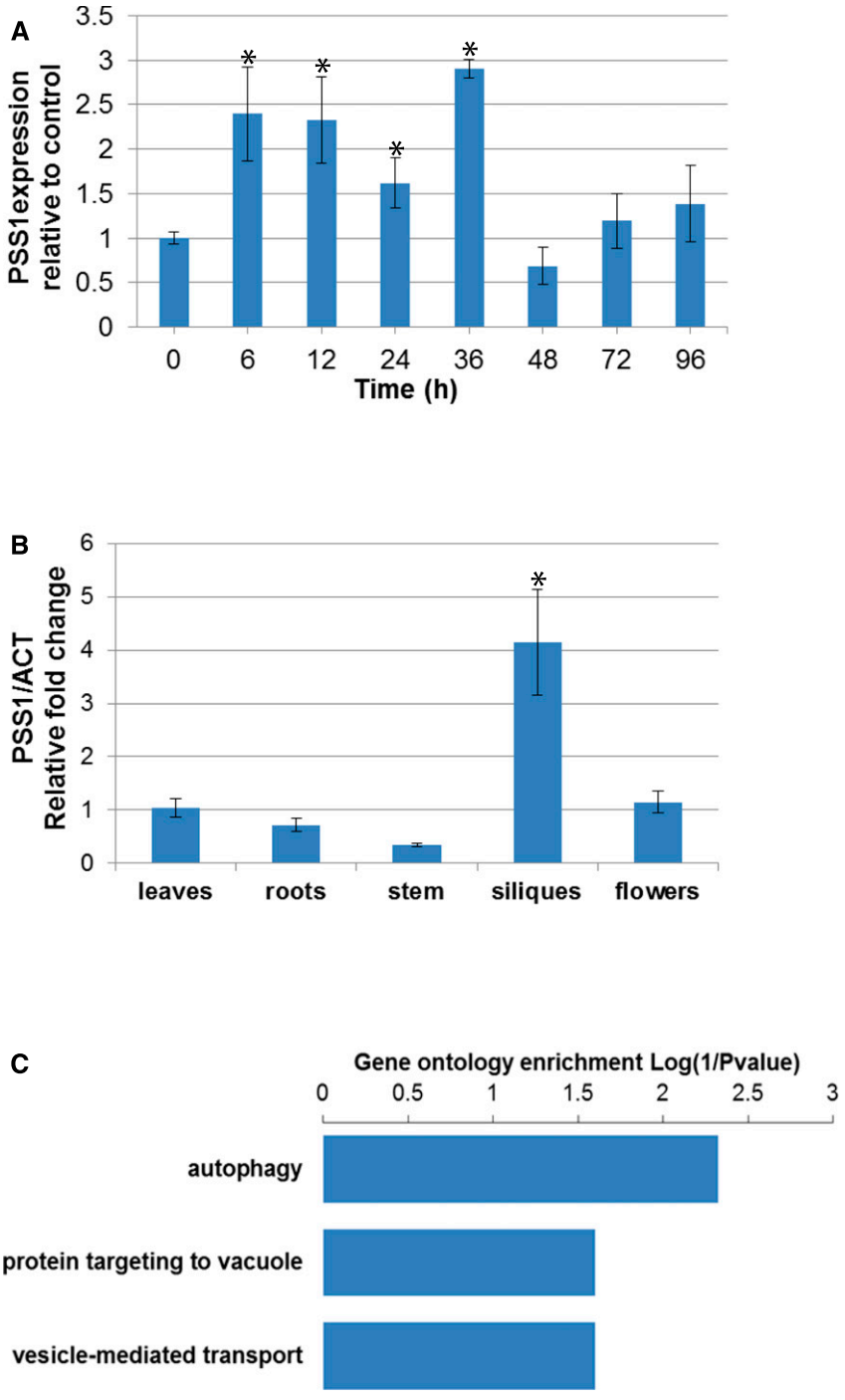

Figure 5. Expression of *PSS1* and genes that show expression patterns similar to *PSS1*. A, Expression of *PSS1* following *P. sojae* infection. qRT-PCR of *PSS1* was conducted following inoculation of Arabidopsis leaves with *P. sojae* in three independent experiments. The fold change values are relative to the mock control. *PSS1* expression levels with asterisks were significantly induced ($P < 0.05$) when compared with the 0-h control. B, Expression patterns of *PSS1* among various Arabidopsis tissues. qRT-PCR expression data of *PSS1* were collected among Arabidopsis organs in three independent experiments. Expression comparison was against the levels in leaves ($P < 0.05$). Data in A and B are from three biological replications, and data were standardized against the transcript levels of the *Actin* gene. C, Gene Ontology enrichment (biological process) of *PSS1* coexpression genes. The coexpression gene analysis was based on the mRNAseq data set using the software Genevestigator (Hruz et al., 2008).

The plasma membrane protein AtPIP2A fused to mCherry was used as a plasma membrane marker (Nelson et al., 2007) and eGFP alone as a control. Two days after coinfiltration, the GFP fluorescence signals of PSS1-GFP were detected as sharp, thin lines at the cell periphery and overlapped with the red fluorescence of the mCherry-fused plasma membrane marker (Fig. 6). After plasmolysis, colocalization of PSS1-GFP with the plasma membrane marker was retained and detached from cell wall, and obvious Hechtian strands were observed (Supplemental Fig. S5B), a characteristic of plasma membrane proteins. These results suggest that PSS1 is most likely an integral plasma membrane protein, not a cell wall protein. The GFP-PSS1 fusion protein with GFP at the N terminus exhibited loss of its plasma membrane localization; instead, it showed cytoplasmic localization, similar to eGFP (Supplemental Fig. S5A). This suggests that the signal for plasma membrane localization in PSS1 is most likely located at the N terminus.

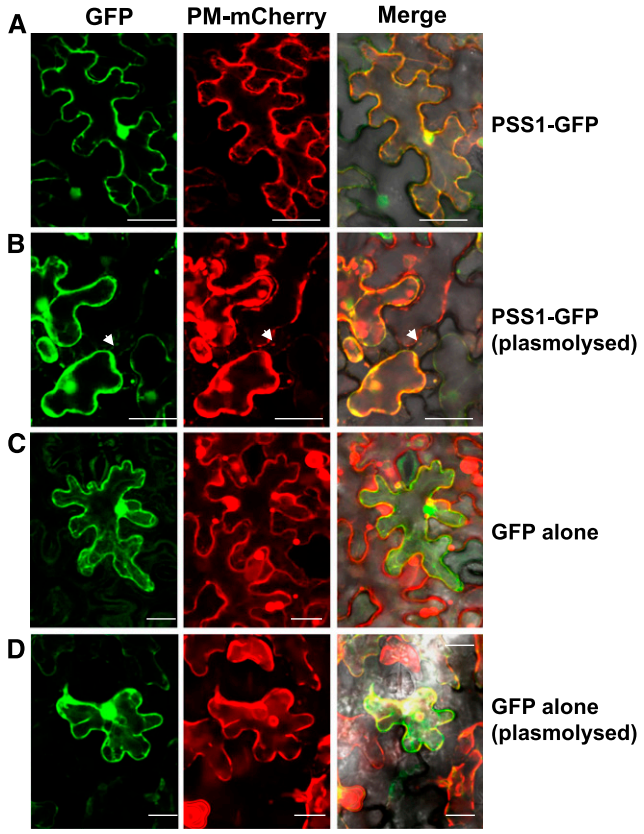

Figure 6. PSS1 is localized to the plasma membrane. A, PSS1-GFP fusion and mCherry-tagged plasma membrane (PM) marker Arabidopsis PIP2A colocalized to plasma membrane of the epidermal cells of *N. benthamiana*. B, The colocalized PSS1-GFP and PIP2A-mCherry fluorescent proteins remain as a complex following plasmolysis with 1 M NaCl. C, Control GFP fluorescent protein was localized to cytoplasm. D, Plasmolysis of the cell coexpressing the GFP and PIP2A-mCherry proteins. White arrowheads indicate Hechtian strands (for details, see Supplemental Fig. S5). Bars = 50 μm for PSS1-GFP and 25 μm for GFP alone.

PSS1 Transgenic Soybean Lines Exhibited Enhanced Sudden Death Syndrome Resistance

The soybean cv Williams 82 was transformed with the *PSS1* cDNA fused individually to three promoters: (1) Prom1, a soybean *F. virguliforme* Mont-1 infection-inducible promoter (*Glyma18g47390*; B.B. Sahu and M.K. Bhattacharyya, unpublished data); (2) Prom2, a soybean root-specific promoter (*Glyma10g31210*; http://www.oardc.ohio-state.edu/SURE/GmROOT/GmRoot.htm; Ngaki et al., 2016); and (3) Ubi10, an Arabidopsis constitutive promoter (*At4g05320*; Norris et al., 1993; Fig. 7A). R1 seeds were collected from R0 soybean plants grown in the greenhouse. Transgenic soybean plants carrying *PSS1* did not show any obvious changes in morphology compared with the nontransgenic recipient cv Williams 82. To examine the responses of transgenic plants to *F. virguliforme*, seeds were planted in a soil premixed with *F. virguliforme* Mont-1 isolate and the seedlings were grown in growth chambers. The cv Williams 82 is a moderately susceptible line, while MN1606 is a sudden death syndrome (SDS)-resistant line. Foliar SDS symptoms were recorded 4 weeks after planting. Approximately one-third to two-thirds of the selected R1 plants showed enhanced SDS resistance, with disease severity ratings of less than 2.0 (Fig. 7B). The nontransgenic cv Williams 82 line exhibited SDS severity ratings of over 4.0 among 90% of the plants, and 90% of MN1606 plants showed disease ratings of less than 2.0. RT-PCR analysis indicated that *PSS1* transcripts were present in all SDS-resistant R1 progeny but not in the SDS-susceptible R1 progeny (Fig. 7C).

Foliar SDS is induced by toxins produced by *F. virguliforme* in infected roots (Ji et al., 2006; Brar et al., 2011). We hypothesized that overexpressed PSS1 in roots conferred enhanced root resistance against the pathogen. To test our hypothesis, seeds of three SDS-resistant R_2 plants, each representing one of the three transgenes (*Prom1-PSS1*, *Prom2-PSS1*, and *Ubi10-PSS1*), were planted in soil mixed with *F. virguliforme* Mont-1 inoculum in a growth chamber. Genomic DNA quantitative PCR (qPCR) was conducted for the single-copy *F. virguliforme FvTox1* toxin gene (Brar et al., 2011). The qPCR revealed that the levels of *F. virguliforme* growth in the roots of SDS-resistant transgenic soybean plants expressing the *PSS1* gene under the control of Prom1, Prom2, or Ubi10 was decreased up to 85% as compared with that in cv Williams 82 (Fig. 7D). These results suggest that PSS1 suppressed the extent of *F. virguliforme*'s spread in the infected roots.

To determine if transgenic SDS-resistant plants showed enhanced SDS resistance under field conditions, field trials were conducted at Hinds Farms, Iowa State University, in the 2015 and 2016 seasons. The transgenic soybean lines carrying *PSS1* transgenes showed enhanced SDS resistance under field conditions (Fig. 8A). In each season, transgenic seeds were planted along with the control lines cv Williams 82, MN1606, or Ripley. The *F. virguliforme* NE305S isolate grown on sorghum (*Sorghum bicolor*) grains was mixed with seeds prior to sowing. In 2015, R1 seeds were sown. Three weeks after seed germination, Basta was sprayed on transgenic lines to eliminate any azygous progeny. We sprayed Basta at early vegetative growth stages. Foliar SDS symptoms appear after flowering, and foliar symptom severity was recorded at the reproductive stage (R6 stage, the stage at which the weight of developing pods peaks). There was a gap of 4 weeks between Basta spray and SDS symptom development. Once symptoms started to appear, the SDS severity of each plant was scored. Transgenic lines, 207-4 and 207-14 expressing Prom2-driven *PSS1*, 227-8 and 227-9 carrying Ubi10 promoter-fused *PSS1*, and 206-7 carrying promoter Prom1-fused *PSS1*, showed significantly enhanced SDS resistance under field conditions ($P < 0.05$; Fig. 8B). Leaves of SDS-resistant plants were collected just after the first scoring of foliar SDS severity to determine the transgene copy number (Supplemental Table S4). The harvested R2 seeds of putative homozygous R1 plants were grown in the 2016 field trial. In 2016, Basta herbicide was applied to eliminate any

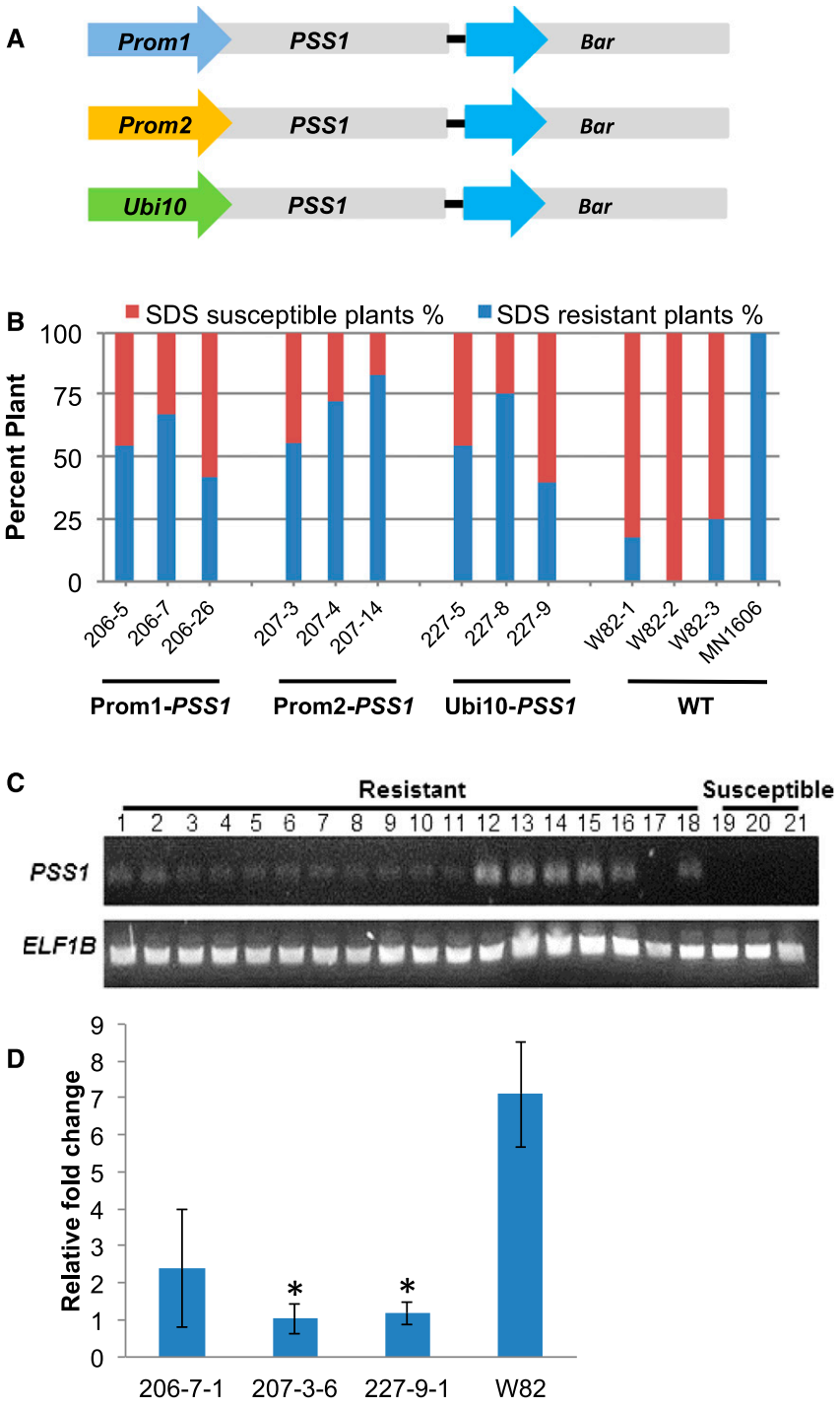

Figure 7. Expression of *PSS1* enhances SDS resistance in transgenic soybean plants under growth chamber conditions. A, Schematic depiction of promoter-*PSS1* fusion genes along with the CaMV 35S promoter-fused *bar* gene in three binary plasmids used to generate transgenic soybean plants. B, Responses of the transgenic lines to root infection with *F. virguliforme* Mont-1 in growth chambers. Plants with foliar SDS scores of 2 or less were considered resistant, and those with scores greater than 2 were considered susceptible. Percentage resistant and susceptible R1 progeny are presented for each of the *PSS1* transgenes generated by fusing the *PSS1* gene to Prom1, Prom2, and Ubi10 promoters. For each transgenic event, 15 R1 plants were studied. The experiment was repeated two more times and showed similar results. Foliar SDS symptoms for individual plants were scored 4 weeks following planting. MN1606, SDS-resistant control; WT, transgene recipient nontransgenic cv Williams 82 (W82) as the SDS-susceptible control. C, RT-PCR analysis of the transgenic R1 plants for *PSS1* transcripts. Lanes 1 to 6, RT-PCR products from *F. virguliforme*-infected roots of three independent lines carrying promoter Prom1 fused to *PSS1*; lanes 7 to 12, RT-PCR products from *F. virguliforme*-infected roots of three independent lines carrying promoter Prom2 fused to *PSS1*; and lanes 13 to18, RT-PCR products from *F. virguliforme*-infected roots of three independent lines carrying promoter Ubi10 fused to *PSS1*. For each independent transgenic line, two R1 SDS-resistant plants (lanes 1–18) were analyzed. Lanes 19 to 21, RT-PCR products from *F. virguliforme*-infected roots of three independent R1 progeny plants that were SDS susceptible. D, Relative biomasses of *F. virguliforme* measured by genomic DNA qPCR of the *FvTox1* gene among three independent transgenic lines. Root samples were collected 2 weeks following infection with the *F. virguliforme* Mont-1 isolate in a growth chamber. 206-7-1, Transgenic line carrying *Prom1-PSS1*; 207-3-6, transgenic line carrying *Prom21-PSS1*; 227-9-1, transgenic line carrying the *Ubi10-1-PSS1* fusion gene; W82, cv Williams 82. Asterisks indicate statistical significance at $P < 0.05$ when compared with the biomass of *F. virguliforme* in cv Williams 82.

possible azygous segregants from heterozygous R1 plants. The SDS severity index indicated that transgenic lines with promoter Prom2- and Ubi10-driven *PSS1* showed enhanced SDS resistance (Fig. 8C).

DISCUSSION

In this investigation, we applied a map-based cloning approach to isolate the Arabidopsis nonhost resistance *PSS1* gene. The gene was mapped to a 2.75-Mb genomic region. A bulked DNA sample of seven $F_{2:3}$ lines homozygous for the *pss1* allele was sequenced to identify the candidate *PSS1* gene through SHORE mapping (Schneeberger et al., 2009). Analyses of T-DNA insertion lines and complementation analyses confirmed that *PSS1* encodes a GRP. Mutations in this gene led to a loss of immunity of Arabidopsis to two soybean pathogens, *P. sojae* and *F. virguliforme*, but not to the bacterial

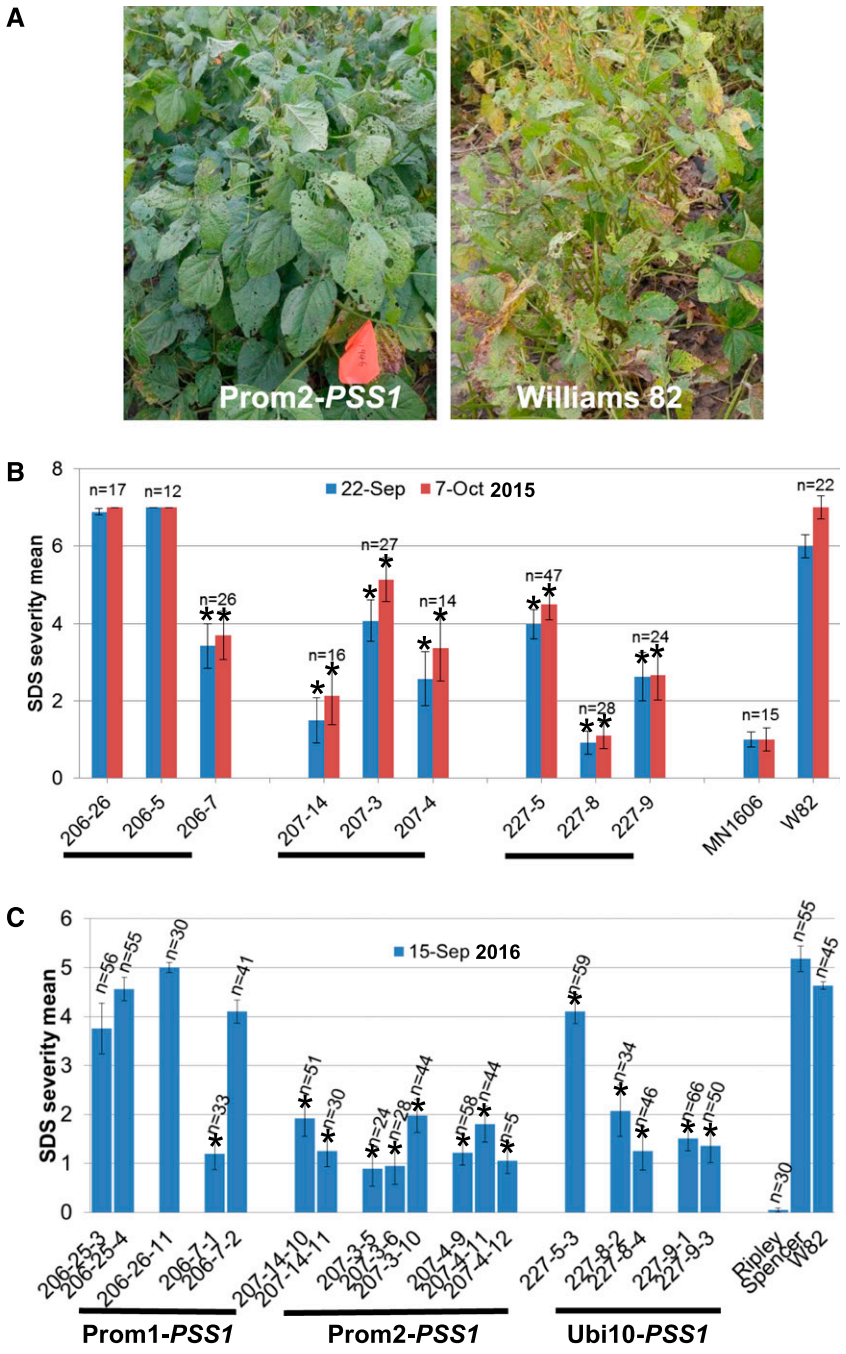

Figure 8. Expression of *PSS1* enhances SDS resistance in transgenic soybean plants under field conditions. A, Representative field plot showing SDS-resistant transgenic and cv Williams 82 control plants. B and C, Mean foliar SDS severity for individual transgenic lines in the 2015 and 2016 field trials. Each line comprised 12 to 66 Basta-resistant R1 or R2 seedlings. The experiment was conducted in a randomized block design. Asterisks indicate significant reductions in foliar SDS scores between transgenic lines and the nontransgenic recipient cv Williams 82 (W82) control at $P < 0.05$.

pathogen, *Pseudomonas syringae* pv *glycinea*, which causes bacterial blight in soybean (Sumit et al., 2012).

The *pss1* mutant was created in the *pen1-1* genetic background because *P. sojae* can penetrate single cells of the *pen1-1* mutant (Sumit et al., 2012). Ecotype Col-0, on the other hand, is not penetrated by *P. sojae*. Therefore, we expected to observe an epistatic effect of PEN1 on PSS1 if PSS1 was to encode a second layer of plant defense. Surprisingly, a 3:1 segregating ratio was observed for the *pss1* mutation (*PSS1*:*pss1*::3:1), suggesting a single gene action with no epistasis effect of PEN1 on PSS1 (Sumit et al., 2012). This observation was further supported by responses of two T-DNA insertion lines, SALK_090245C and SALK_148857C. Both mutants are susceptible to *P. sojae*, although both carry the *PEN1* allele (Fig. 2). Together with the previous study (Sumit et al., 2012), our study suggests that PSS1 may act at both prehaustorial and posthaustorial levels, while PEN1 acts at the prehaustorial level against this soybean pathogen.

PSS1 encodes GRP1. GRPs are classified into seven classes based on the pattern of their Gly-rich domain.

PSS1 belongs to group VII, which carry a mixed arrangement of Gly repeats with no other conserved domains (Mangeon et al., 2010).

PSS1 confers broad-spectrum nonhost immunity of Arabidopsis to two soybean pathogens (Sumit et al., 2012). Transgenic studies in soybean have suggested the utility of this gene in enhancing disease resistance in crop plants. We have localized the protein to the plasma membrane through its transient expression in *N. benthamiana* (Fig. 6). The broad-spectrum disease resistance function and its putative plasma membrane location suggest a possible recognition/signaling role for the protein in the activation of host defense responses. However, we cannot rule out the possibility of other mechanisms, including possible structural and/or chemical barriers mediated by PSS1.

GRPs are involved in multiple functions in the plant defense response, such as blocking virus movement, interacting with kinases, and modulating the transcription of defense genes (Park et al., 2001, 2008; Ueki and Citovsky, 2002, 2005; Tao et al., 2006; Kim et al., 2007, 2015; Nicaise et al., 2013). *PSS1* is induced by many pathogens. PAMPs such as flagellin (flg22), harpin (HrpZ), necrosis-inducing proteins, and lipopolysaccharide also can induce its expression. Surprisingly, the bacterial PAMP HrpZ is Gly rich and triggers the hypersensitive response at the infection site (Choi et al., 2013).

The subcellular localization and predicted protein structure suggest that PSS1 is an integral plasma membrane protein carrying one membrane-spanning domain. Plant immunity is regulated at both transcriptional and posttranscriptional levels. Pre-RNAs of target regulatory genes must be processed correctly to regulate defense responses. GRPs with an RNA-binding domain have been suggested to play a role in RNA processing (Woloshen et al., 2011). Alternate splicing has been documented as essential for the expression of effector-triggered immunity in tobacco (Dinesh-Kumar and Baker, 2000). Whether PSS1 has any role in RNA splicing has yet to be investigated.

The functions of coexpressed genes showing the same transcriptional regulatory pathway could be used in predicting the functions of genes. RT-PCR of seven genes that were coexpressed with *PSS1* in mRNA sequencing or transcript hybridization to microarrays studies indicated that *PSS1* coexpresses with the core autophagy gene *ATG8a* (*At4g21980*; Supplemental Table S3; Yoshimoto et al., 2004). Autophagy is a conserved intracellular trafficking and degradation process and has been shown to be linked to the induction of programmed cell death or the hypersensitive response as part of basal plant immunity (Liu et al., 2005; Teh and Hofius, 2014). It will be important to determine if PSS1 is involved in autophagy-mediated plant immunity.

In recent years, SDS has emerged as the second most serious soybean disease after soybean cyst nematodes in the United States; in certain years, it can cause yield suppression valued up to $0.7 billion (Bradley and Allen, 2014). Although first reported in 1971, the fungal pathogen *F. virguliforme* causing SDS has spread to all soybean-growing states in the United States and Canada (Ngaki et al., 2016). Currently, the use of SDS-resistant cultivars is the only option available to manage this disease. However, breeding SDS-resistant cultivars is not trivial, since the SDS resistance is partial and governed by more than 40 quantitative trait loci (Swaminathan et al., 2016). The pathogen is soil borne and remains in infected roots, where it produces toxins that cause the foliar SDS (Brar et al., 2011; Brar and Bhattacharyya, 2012; Pudake et al., 2013; Chang et al., 2016). The development of transgenic SDS-resistant lines is a possible alternative to combat this disease. The transgenic expression of plant antibodies or interacting peptides that bind to foliar SDS-inducing toxins has shown some promise in enhancing SDS resistance in soybean (Brar and Bhattacharyya, 2012; Wang et al., 2015; B. Wang and M.K. Bhattacharyya, unpublished data).

Our study suggests that nonhost disease resistance governed by *PSS1* can enhance SDS resistance in transgenic soybean plants by restricting the spread of fungal growth in the infected roots (Fig. 7D). It is very unlikely that the enhanced SDS resistance in the transgenic lines was induced by Basta spray, as was observed in an earlier study conducted in transgenic rice (*Oryza sativa*; Ahn, 2008), because of the following reasons. In the growth chamber assays, we never sprayed Basta (Fig. 7). Second, although we sprayed Basta in both the 2015 and 2016 growing seasons on the field-grown soybean plants, not all transgenic soybean lines were SDS resistant; some were as susceptible as the nontransgenic cv Williams 82 plants (Fig. 8).

The *PSS1*-encoded resistance mechanism could complement the natural SDS resistance mechanisms and be suitable in breeding SDS-resistant soybean lines. Considering the widespread cultivation of transgenic soybean worldwide (e.g. about 94% of the soybean crop grown in the United States and 81% worldwide are transgenic; Perry et al., 2016), the development of SDS-resistant transgenic plants could be a good alternative to facilitate soybean breeding programs for SDS resistance.

In summary, *PSS1* encodes a novel unknown mechanism to confer nonhost resistance of Arabidopsis against two important soybean pathogens, *P. sojae* and *F. virguliforme*. Its plasma membrane localization and induction in response to infection by multiple pathogens and treatment with PAMPs suggest its possible regulatory role in plant defenses. It is possible that PSS1 may confer its plant immunity function through autophagy. The transgenic study of *PSS1* revealed that the transfer of nonhost resistance genes could be an important strategy in engineering disease resistance in crop plants.

MATERIALS AND METHODS

Plants and Pathogens

Arabidopsis (*Arabidopsis thaliana*) plants including the wild-type ecotypes Col-0 and Niederzenz as well as mutants were grown on LC1 soil (Sun Gro

Horticulture) in growth chambers at 21°C and 60% humidity with a dark/light cycle of 8/16 h and a light intensity of 100 μmol m^{-2} s^{-1}. Soybean (*Glycine max*) 'Williams 82' and transgenic lines were grown on Metro Mix 910 (Sun Gro Horticulture) at 23°C and 60% humidity with a dark/light cycle of 8/16 h and a light intensity of 300 μmol m^{-2} s^{-1} in growth chambers. The *Phytophthora sojae* NW strain was maintained on V8 agar plates, and *Fusarium virguliforme* isolates were maintained on PDA plates.

Nonhost-Resistant Gene Cloning

The *PSS1* gene was mapped previously to the lower arm of chromosome 3 between markers SBP_20.71 and SBP_23.46 by conducting bulked segregation analysis in a segregating population developed from a cross between the *pss1* mutant and Niederzenz (Sumit et al., 2012). Subsequently, genomic DNA of seven homozygous susceptible *pss1*/*pss1* $F_{2:3}$ families was extracted using the CTAB method (Murray and Thompson, 1980) and bulked for sequencing on the Illumina HiSeq 2500 platform at the Iowa State University DNA Facility. The short sequencing reads were assembled into contigs, which were aligned to the reference Col-0 sequence to identify mutations in the 2.75-Mb *pss1* region using the SHORE program (Schneeberger et al., 2009). Because the *pss* mutants were developed in the *pen1-1* mutant, any mutations originating from *pen1-1* were not considered for further analysis.

Homozygous T-DNA knockout lines for the candidate *PSS1* genes carrying nonsynonymous mutations were obtained from the Arabidopsis Biological Resource Center located at Ohio State University, and individual T-DNA mutant lines were verified by PCR amplification (Supplemental Table S1). Leaves of 3-week-old T-DNA insertion mutant lines, *pss1*, *pen1-1*, and Col-0 plants were inoculated with 20 μL of *P. sojae* NW zoospores (5×10^5 mL^{-1}) as described previously (Sumit et al., 2012). Symptoms were scored 3 and 4 d after inoculation.

To complement *pss1* and T-DNA insertion mutant lines, the nonhost-resistant cDNA was amplified by RT-PCR from the Col-0 transcripts and inserted into the binary vector pTF101.1 under the control of the CaMV 35S promoter. Sequencing was performed to confirm the identity of the *PSS1* gene. The resulting construct was transformed into *Agrobacterium tumefaciens* strain EHA101 by following the freeze-thaw method. *pss1* and T-DNA insertion mutant lines were transformed by conducting floral dip of the mutants with the *A. tumefaciens* EHA101 isolate carrying the candidate *PSS1* gene (Weigel and Glazebrook, 2006). T1 and T2 progeny were screened for Basta resistance by spraying with Liberty (80 μg mL^{-1}) herbicide. T3 plants along with the controls Col-0, *pss1* mutant, and T-DNA insertion lines were inoculated with *P. sojae* spores to examine their disease phenotypes.

qRT-PCR

For qRT-PCR analyses of the *PSS1* gene, three leaves of 3-week-old *pss1* mutant plants were inoculated with 20 μL of *P. sojae* NW zoospores (5×10^5 mL^{-1}) or water. Leaf samples were collected 6, 12, 24, 36, 48, 72, and 96 h after inoculation in three independent experiments. Total RNA was extracted using the SV Total RNA isolation kit (Promega). The isolated RNAs were reverse transcribed into cDNA using the SuperScript first-strand synthesis system (Thermo Fisher Scientific). Transcript amounts of the *PSS1* and *Actin* genes were examined by conducting qRT-PCR with *PSS1*- and *Actin*-specific primers (Supplemental Table S5). qRT-PCR was conducted using SYBR Green master mixes (Thermo Fisher Scientific) by following the manufacturer's instruction manual. For the study of tissue-specific expression of *PSS1* in various tissues, including stem, roots, flowers, leaves, and siliques, RNA extraction was conducted as described earlier for leaves. The induced fold changes in *PSS1* expression were calculated against the mock control.

To quantify the pathogen biomass in infected soybean roots, a genomic DNA-PCR was conducted for the DNA isolated from the transgenic and nontransgenic cv Williams 82 soybean plants infected with *F. virguliforme* Mont-1. DNA was diluted to 20 ng μL^{-1} for qPCR to quantify the single-copy *F. virguliforme FvTox1* gene (Brar et al., 2011) as a measure of fungal biomass. The single-copy soybean gene, *Glyma.05G014200*, was used as an internal control. qPCR was run in an iQ5 Bio-Rad instrument using the SYBR Green protocol. The primers used for qPCR of *Glyma.05G014200* were evaluated earlier (Ngaki et al., 2016) and are presented in Supplemental Table S5. For qPCR of *FvTox1*, primers developed previously for the quantification of *FvTox1* and *F. virguliforme* biomass were used (Mbofung et al., 2011; Supplemental Table S5).

RT-PCR

To investigate the expression of *PSS1* and identified genes that are coexpressed with *PSS1*, leaves of Col-0 and *pss1* were inoculated with 20 μL of *P. sojae* NW isolate zoospore suspension (10^5 zoospores mL^{-1}). Inoculated leaves were harvested in a time course (0, 6, 12, and 24 h postinoculation), and the RNAs were isolated and subjected to RT-PCR using primers specific for each gene (Supplemental Table S5). The Arabidopsis *Actin* gene was used as an internal control. The intensity of PCR bands of individual samples was quantified by using ImageJ (http://rsb.info.nih.gov/ij/index.html). We followed the procedure outlined in the ImageJ document to collect the pixelated data (https://imagej.nih.gov/ij/docs/user-guide-A4booklet.pdf, p. 129). The data from three independent experiments were analyzed for statistically significant differences for *P. sojae*-infected and uninfected water control leaf tissues for eight genes, including *PSS1*, using the open-source R program (Supplemental Table S3).

Subcellular Localization of PSS1

The *PSS1* gene was fused at the N and C termini of GFP and cloned in pISUAgron5 vector (S. Li, N.N. Narayanan, and M.K. Bhattacharyya, unpublished data), in which *eGFP* is already fused to the CaMV 35S promoter. pISUAgron5 vector was used as the GFP control. A plasma membrane marker, Arabidopsis PIP2A fused to the mCherry tag, was obtained from the Arabidopsis Biological Resource Center (Nelson et al., 2007). For *A. tumefaciens*-mediated transient transformation, individual *A. tumefaciens* isolates containing each of the two GFP fusion constructs or control GFP construct were coinfiltrated with plasma membrane marker into leaves of 4-week-old *Nicotiana benthamiana* plants (Shamloul et al., 2014). Two days following infiltration, small leaf pieces were mounted in either water or 1 M NaCl. Samples were observed with a 20× oil-immersion lens mounted to a Leica SP5 X MP confocal/multiphoton inverted microscope. To monitor GFP fluorescence, a 488-nm argon laser and PMT detector with emission bandwidth set to 495 to 550 nm were used. To monitor the mCherry signal, a HeNe 561 laser (561 nm) and a third PMT detector (587–610 nm) were used (Schweiger and Schwenkert, 2014).

Generation of Transgenic Soybean Lines

The gene *PSS1* was first cloned into vector pGEM-T (Promega) and sequenced to confirm its identity. The gene was then released from the pGEM-T vector and cloned in the modified binary pTF102 vectors carrying one of three promoters: Prom1, Prom2, and Ubi10. Prom1 is a soybean infection-inducible promoter (*Glyma18g47390*; B.B. Sahu and M.K. Bhattacharyya, unpublished data). Prom2 is a soybean root-specific promoter (*Glyma10g31210*; http://www.oardc.ohio-state.edu/SURE/GmROOT/GmRoot.htm; Ngaki et al., 2016). The Ubi10 promoter was isolated from the Arabidopsis *At4g05320* gene (Norris et al., 1993). The resulting three constructs were transformed into *A. tumefaciens* strain EHA101 to generate stable transformants in the soybean cv Williams 82 at the Plant Transformation Facility, Iowa State University (Paz et al., 2004). Basta (glufosinate)-resistant R0 plants were tested for incorporation of the *bar* gene by PCR. For each *PSS1* construct, at least three transgenic events were generated. Basta-resistant R0 plants were grown in a greenhouse to maturity for harvesting R1 seeds.

Evaluation of *PSS1* Transgenic Lines in a Growth Chamber and under Field Conditions for SDS Resistance

R1 progeny derived from self-pollinated R0 plants were investigated for possible enhanced SDS resistance under growth chamber conditions. The *F. virguliforme* inocula were prepared, and colony-forming units of the inocula were determined as described previously (Li et al., 2009). To prepare the inoculum, 500 g of sorghum (*Sorghum bicolor*) grains was first soaked in distilled water overnight and then washed five times to remove sorghum seeds and debris that were floated. The excess water was drained, and grains were autoclaved for 40 min at 121°C. Each of the flasks containing sterilized sorghum grains was inoculated with *F. virguliforme* isolate Mont-1 by transferring 10 20-mm-diameter plugs from one-third-strength PDA plates containing 2-week-old *F. virguliforme* Mont-1 culture. Flasks were then incubated at room light and temperature and shaken gently by hand every other day for 2 weeks to ensure uniform fungal growth. After 1 month, the sorghum grains, infested with the fungus, were dried for 24 h under a fume hood. Infested kernels were then stored at 4°C until further use, typically no longer than 3 months.

For growth chamber assays, a 2:1 mixture of sand and soil was mixed with the inocula at a ratio of 19:1::soil mix:inocula and placed in 237-mL Styrofoam cups for sowing three seeds of each genotype. Fifteen seeds of each soybean line were evaluated in five Styrofoam cups. Plants were grown in a growth chamber at 22°C to 23°C and with light intensity of 300 μmol photons m^{-2} s^{-1} (Luckew et al., 2013). Foliar symptoms were scored 3 and 4 weeks following planting (Hartman et al., 1997).

R1 and R2 seeds were evaluated in field trials in two consecutive seasons, from June 11 to October 30, 2015, and from June 1 to October 15, 2016, at Hinds Research Farm, Iowa State University, located 4 miles north of Ames, Iowa. Field trials were carried out using a completely randomized block design with two replications in the 2015 trial and three replications in the 2016 trial. Twenty-four seeds of each genotype were mixed with approximately 5 mL of inocula of the *F. virguliforme* NE305S isolate and sown using a hand-push planter. At the unifoliate stage, transgenic lines were sprayed with glufosinate herbicide (250 mg L^{-1}) mixed with 0.1% Tween 20. The spray was repeated 3 d later. The field was heavily irrigated to generate favorable conditions for SDS symptom development. In the 2016 trial, only homozygous transgenic lines showing 100% herbicide resistance were scored for foliar SDS. Individual plants were scored for foliar SDS symptoms using a scale of 1 to 7 (modified from Hartman et al., 1997) as follows: 1, no symptoms; 2, slight symptom development, with mottling and mosaic on leaves (1%–20% foliage affected); 3, moderate symptom development, with interveinal chlorosis and necrosis on foliage (21%–50% foliage affected); 4, heavy symptom development, with interveinal chlorosis and necrosis (51%–80% foliage affected); 5, severe interveinal chlorosis and necrosis (81%–100% foliage affected); 6, whole leaf necrosis; and 7, death of plants.

Molecular Characterization of Transgenic Plants

To verify gene expression in transgenic lines or Arabidopsis lines, total RNA was extracted using the SV Total RNA isolation system (Promega), following the manufacturer's instructions, and quantified using a NanoDrop ND-1000 spectrophotometer (Thermo Scientific). The isolated RNAs were reverse transcribed into cDNAs using the SuperScript first-strand synthesis system for RT-PCR (Thermo Fisher Scientific). Semiquantitative RT-PCR was conducted for the *PSS1* gene or coexpressed genes along with *ELF1B* as the internal control.

Transgene copy numbers were determined by qPCR. Young leaves of transgenic plants were collected in the field, and genomic DNA was extracted at the Iowa State University DNA Facility using the Autogenprep 740 DNA extraction robot (AutoGen). The DNA amount of each sample was measured with a NanoDrop spectrophotometer and then was diluted to 20 ng μL^{-1} for qPCR. qPCR was conducted on a Biomark HD system using the 192.24 Taqman CNV protocol (Fluidigm). Two Taqman assays were designed (Supplemental Table S5): the *bar* gene (target) and the reference gene (an endogenous single-copy gene, *Glyma.05G014200*). Reporter/quencher dyes used were FAM/MGB-NFQ for *bar* and VIC/TAMRA for the reference gene. Data were analyzed using a Biomark HD data collection software, and from the analyzed data, the copy number for the *bar* gene was calculated.

Statistical Analysis

All data are presented as means ± SE from at least three biological replications. The statistical significance of the difference was determined by conducting Student's *t* test. Differences between treatments were considered significant at $P < 0.05$ in a two-tailed test. The statistical analysis for significant differences also was conducted using the open-source R program.

Bioinformatics Analyses

The conserved motifs in the PSS1 protein were predicated using the MyHits program (http://myhits.isb-sib.ch/cgi-bin/motif_scan). The prediction of signal peptide was conducted using SignalP 4.0 (Petersen et al., 2011). The transmembrane domain was predicted at the TMHMM Server version 2.0 (http://www.cbs.dtu.dk/services/TMHMM/). Genes coexpressed with *PSS1* were identified from the ATTED-II database (http://atted.jp/) and Genevestigator (Hruz et al., 2008) using microarray and mRNAseq data sets, respectively. The phylogenetic tree of PSS1 homologs was generated by the neighbor-joining method with 1,000 bootstrap replications using the MEGA7 program (Kumar et al., 2016). Protein structure prediction of PSS1 and its mutant and their pairwise structure alignment were accomplished by using the I-TASSER and TM-align programs, respectively (http://zhanglab.ccmb.med.umich.edu/).

Supplemental Data

The following supplemental materials are available.

Supplemental Figure S1. Complementation analysis of the *pss1* mutant with the CaMV 35S promoter-fused *PSS1* cDNA.

Supplemental Figure S2. Structure comparison of PSS1 and its mutant pss1 protein.

Supplemental Figure S3. Alignment of PSS1 homologs.

Supplemental Figure S4. Coexpression gene analysis based on the microarray data set.

Supplemental Figure S5. Subcellular localization of N- or C-terminal GFP-tagged PSS1.

Supplemental Table S1. T-DNA insertional lines used for the identification of the candidate *PSS1* gene.

Supplemental Table S2. Top 15 biotic stresses that induce the expression of *PSS1*.

Supplemental Table S3. Induction of the gene (*At4g21980*) encoding an autophagy-related protein 8A coexpressed with *PSS1* in *pss1*.

Supplemental Table S4. *pss1* transgene copy number among the R1 plants.

Supplemental Table S5. Primers used in this study.

ACKNOWLEDGMENTS

We thank David Grant for reviewing the article and Jordan Baumbach for contributions in managing soybean transgenic plants; we also thank the Iowa State University Plant Transformation Facility for the generation of transgenic soybean plants and the Iowa State University DNA Facility for sequencing and preparation of soybean DNA samples.

Received May 9, 2017; accepted September 21, 2017; published September 26, 2017.

LITERATURE CITED

Ahn IP (2008) Glufosinate ammonium-induced pathogen inhibition and defense responses culminate in disease protection in bar-transgenic rice. Plant Physiol **146:** 213–227

Alonso JM, Stepanova AN, Leisse TJ, Kim CJ, Chen H, Shinn P, Stevenson DK, Zimmerman J, Barajas P, Cheuk R, et al (2003) Genome-wide insertional mutagenesis of *Arabidopsis thaliana*. Science **301:** 653–657

Ballouz S, Verleyen W, Gillis J (2015) Guidance for RNA-seq co-expression network construction and analysis: safety in numbers. Bioinformatics **31:** 2123–2130

Bradley C, Allen T (2014) Estimates of soybean yield reductions caused by diseases in the United States. http://extension.cropsciences.illinois.edu/fieldcrops/diseases/ yield_reductions.php (November 1, 2017)

Brar HK, Bhattacharyya MK (2012) Expression of a single-chain variable-fragment antibody against a *Fusarium virguliforme* toxin peptide enhances tolerance to sudden death syndrome in transgenic soybean plants. Mol Plant Microbe Interact **25:** 817–824

Brar HK, Swaminathan S, Bhattacharyya MK (2011) The *Fusarium virguliforme* toxin FvTox1 causes foliar sudden death syndrome-like symptoms in soybean. Mol Plant Microbe Interact **24:** 1179–1188

Campe R, Langenbach C, Leissing F, Popescu GV, Popescu SC, Goellner K, Beckers GJM, Conrath U (2016) ABC transporter PEN3/PDR8/ABCG36 interacts with calmodulin that, like PEN3, is required for Arabidopsis nonhost resistance. New Phytol **209:** 294–306

Chang HX, Domier LL, Radwan O, Yendrek CR, Hudson ME, Hartman GL (2016) Identification of multiple phytotoxins produced by *Fusarium virguliforme* including a phytotoxic effector (FvNIS1) associated with sudden death syndrome foliar symptoms. Mol Plant Microbe Interact **29:** 96–108

Choi MS, Kim W, Lee C, Oh CS (2013) Harpins, multifunctional proteins secreted by gram-negative plant-pathogenic bacteria. Mol Plant Microbe Interact **26:** 1115–1122

Clay NK, Adio AM, Denoux C, Jander G, Ausubel FM (2009) Glucosinolate metabolites required for an Arabidopsis innate immune response. Science **323:** 95–101

Collins NC, Thordal-Christensen H, Lipka V, Bau S, Kombrink E, Qiu JL, Hückelhoven R, Stein M, Freialdenhoven A, Somerville SC, et al (2003) SNARE-protein-mediated disease resistance at the plant cell wall. Nature **425:** 973–977

Dinesh-Kumar SP, Baker BJ (2000) Alternatively spliced N resistance gene transcripts: their possible role in tobacco mosaic virus resistance. Proc Natl Acad Sci USA **97:** 1908–1913

Egorov TA, Odintsova TI, Pukhalsky VA, Grishin EV (2005) Diversity of wheat anti-microbial peptides. Peptides **26:** 2064–2073

Fu ZQ, Guo M, Jeong BR, Tian F, Elthon TE, Cerny RL, Staiger D, Alfano JR (2007) A type III effector ADP-ribosylates RNA-binding proteins and quells plant immunity. Nature **447:** 284–288

Hadwiger LA (2015) Anatomy of a nonhost disease resistance response of pea to *Fusarium solani*: PR gene elicitation via DNase, chitosan and chromatin alterations. Front Plant Sci **6:** 373

Hartman GL, Huang YH, Nelson RL, Noel GR (1997) Germplasm evaluation of Glycine max for resistance to *Fusarium solani*, the causal organism of sudden death syndrome. Plant Dis **81:** 515–518

Heath MC (2000) Nonhost resistance and nonspecific plant defenses. Curr Opin Plant Biol **3:** 315–319

Hruz T, Laule O, Szabo G, Wessendorp F, Bleuler S, Oertle L, Widmayer P, Gruissem W, Zimmermann P (2008) Genevestigator v3: a reference expression database for the meta-analysis of transcriptomes. Adv Bioinformatics **2008:** 420747

Ji J, Scott MP, Bhattacharyya MK (2006) Light is essential for degradation of ribulose-1,5-bisphosphate carboxylase-oxygenase large subunit during sudden death syndrome development in soybean. Plant Biol (Stuttg) **8:** 597–605

Jones JDG, Dangl JL (2006) The plant immune system. Nature **444:** 323–329

Kanehisa M, Goto S (2000) KEGG: Kyoto Encyclopedia of Genes and Genomes. Nucleic Acids Res **28:** 27–30

Kerrien S, Alam-Faruque Y, Aranda B, Bancarz I, Bridge A, Derow C, Dimmer E, Feuermann M, Friedrichsen A, Huntley R, et al (2007) IntAct: open source resource for molecular interaction data. Nucleic Acids Res **35:** D561–D565

Kim DS, Kim NH, Hwang BK (2015) GLYCINE-RICH RNA-BINDING PROTEIN1 interacts with RECEPTOR-LIKE CYTOPLASMIC PROTEIN KINASE1 and suppresses cell death and defense responses in pepper (*Capsicum annuum*). New Phytol **205:** 786–800

Kim JY, Park SJ, Jang B, Jung CH, Ahn SJ, Goh CH, Cho K, Han O, Kang H (2007) Functional characterization of a glycine-rich RNA-binding protein 2 in *Arabidopsis thaliana* under abiotic stress conditions. Plant J **50:** 439–451

Kumar S, Stecher G, Tamura K (2016) MEGA7: Molecular Evolutionary Genetics Analysis version 7.0 for bigger datasets. Mol Biol Evol **33:** 1870–1874

Langenbach C, Campe R, Schaffrath U, Goellner K, Conrath U (2013) UDP-glucosyltransferase UGT84A2/BRT1 is required for Arabidopsis nonhost resistance to the Asian soybean rust pathogen *Phakopsora pachyrhizi*. New Phytol **198:** 536–545

Lee S, Whitaker VM, Hutton SF (2016) Potential applications of non-host resistance for crop improvement. Front Plant Sci **7:** 997

Li S, Hartman GL, Chen Y (2009) Evaluation of aggressiveness of *Fusarium virguliforme* isolates that cause soybean sudden death syndrome. J Plant Pathol **91:** 77–86

Lin CH, Chen CY (2014) Characterization of the dual subcellular localization of *Lilium* LsGRP1, a plant class II glycine-rich protein. Phytopathology **104:** 1012–1020

Lipka V, Dittgen J, Bednarek P, Bhat R, Wiermer M, Stein M, Landtag J, Brandt W, Rosahl S, Scheel D, et al (2005) Pre- and postinvasion defenses both contribute to nonhost resistance in Arabidopsis. Science **310:** 1180–1183

Liu Y, Schiff M, Czymmek K, Tallóczy Z, Levine B, Dinesh-Kumar SP (2005) Autophagy regulates programmed cell death during the plant innate immune response. Cell **121:** 567–577

Luckew AS, Leandro LF, Bhattacharyya MK, Nordman DJ, Lightfoot DA, Cianzio SR (2013) Usefulness of 10 genomic regions in soybean associated with sudden death syndrome resistance. Theor Appl Genet **126:** 2391–2403

Mangeon A, Junqueira RM, Sachetto-Martins G (2010) Functional diversity of the plant glycine-rich proteins superfamily. Plant Signal Behav **5:** 99–104

Mbofung GCY, Fessehaie A, Bhattacharyya MK, Leandro LFS (2011) A new TaqMan real-time polymerase chain reaction assay for quantification of *Fusarium virguliforme* in soil. Plant Dis **95:** 1420–1426

Mellersh DG, Heath MC (2003) An investigation into the involvement of defense signaling pathways in components of the nonhost resistance of *Arabidopsis thaliana* to rust fungi also reveals a model system for studying rust fungal compatibility. Mol Plant Microbe Interact **16:** 398–404

Mousavi A, Hotta Y (2005) Glycine-rich proteins: a class of novel proteins. Appl Biochem Biotechnol **120:** 169–174

Murray MG, Thompson WF (1980) Rapid isolation of high molecular weight plant DNA. Nucleic Acids Res **8:** 4321–4325

Mysore KS, Ryu CM (2004) Nonhost resistance: how much do we know? Trends Plant Sci **9:** 97–104

Nakao M, Nakamura R, Kita K, Inukai R, Ishikawa A (2011) Non-host resistance to penetration and hyphal growth of *Magnaporthe oryzae* in Arabidopsis. Sci Rep **1:** 171

Nelson BK, Cai X, Nebenführ A (2007) A multicolored set of in vivo organelle markers for co-localization studies in Arabidopsis and other plants. Plant J **51:** 1126–1136

Ngaki MN, Wang B, Sahu BB, Srivastava SK, Farooqi MS, Kambakam S, Swaminathan S, Bhattacharyya MK (2016) Tanscriptomic study of the soybean-*Fusarium virguliforme* interaction revealed a novel ankyrin-repeat containing defense gene, expression of whose during infection led to enhanced resistance to the fungal pathogen in transgenic soybean plants. PLoS ONE **11:** e0163106

Nicaise V, Joe A, Jeong BR, Korneli C, Boutrot F, Westedt I, Staiger D, Alfano JR, Zipfel C (2013) *Pseudomonas* HopU1 modulates plant immune receptor levels by blocking the interaction of their mRNAs with GRP7. EMBO J **32:** 701–712

Norris SR, Meyer SE, Callis J (1993) The intron of *Arabidopsis thaliana* polyubiquitin genes is conserved in location and is a quantitative determinant of chimeric gene expression. Plant Mol Biol **21:** 895–906

Obayashi T, Kinoshita K, Nakai K, Shibaoka M, Hayashi S, Saeki M, Shibata D, Saito K, Ohta H (2007) ATTED-II: a database of co-expressed genes and cis elements for identifying co-regulated gene groups in Arabidopsis. Nucleic Acids Res **35:** D863–D869

Ortega-Amaro MA, Rodríguez-Hernández AA, Rodríguez-Kessler M, Hernández-Lucero E, Rosales-Mendoza S, Ibáñez-Salazar A, Delgado-Sánchez P, Jiménez-Bremont JF (2015) Overexpression of AtGRDP2, a novel glycine-rich domain protein, accelerates plant growth and improves stress tolerance. Front Plant Sci **5:** 782

Park AR, Cho SK, Yun UJ, Jin MY, Lee SH, Sachetto-Martins G, Park OK (2001) Interaction of the Arabidopsis receptor protein kinase Wak1 with a glycine-rich protein, AtGRP-3. J Biol Chem **276:** 26688–26693

Park CJCB, Park CB, Hong SS, Lee HS, Lee SY, Kim SC (2000) Characterization and cDNA cloning of two glycine- and histidine-rich antimicrobial peptides from the roots of shepherd's purse, *Capsella bursa-pastoris*. Plant Mol Biol **44:** 187–197

Park JH, Suh MC, Kim TH, Kim MC, Cho SH (2008) Expression of glycine-rich protein genes, *AtGRP5* and *AtGRP23*, induced by the cutin monomer 16-hydroxypalmitic acid in *Arabidopsis thaliana*. Plant Physiol Biochem **46:** 1015–1018

Paz MM, Shou H, Guo Z, Zhang Z, Banerjee AK, Wang K (2004) Assessment of conditions affecting *Agrobacterium*-mediated soybean transformation using the cotyledonary node explant. Euphytica **136:** 167–179

Perry ED, Ciliberto F, Hennessy DA, Moschini G (2016) Genetically engineered crops and pesticide use in U.S. maize and soybeans. Sci Adv **2:** e1600850

Petersen TN, Brunak S, von Heijne G, Nielsen H (2011) SignalP 4.0: discriminating signal peptides from transmembrane regions. Nat Methods **8:** 785–786

Pudake RN, Swaminathan S, Sahu BB, Leandro LF, Bhattacharyya MK (2013) Investigation of the *Fusarium virguliforme fvtox1* mutants revealed that the FvTox1 toxin is involved in foliar sudden death syndrome development in soybean. Curr Genet **59:** 107–117

Rhee SY, Beavis W, Berardini TZ, Chen G, Dixon D, Doyle A, Garcia-Hernandez M, Huala E, Lander G, Montoya M, et al (2003) The Arabidopsis Information Resource (TAIR): a model organism database providing a centralized, curated gateway to Arabidopsis biology, research materials and community. Nucleic Acids Res **31:** 224–228

Schneeberger K, Ossowski S, Lanz C, Juul T, Petersen AH, Nielsen KL, Jørgensen JE, Weigel D, Andersen SU (2009) SHOREmap: simultaneous mapping and mutation identification by deep sequencing. Nat Methods **6:** 550–551

Schulze-Lefert P, Panstruga R (2011) A molecular evolutionary concept connecting nonhost resistance, pathogen host range, and pathogen speciation. Trends Plant Sci **16:** 117–125

Schweiger R, Schwenkert S (2014) Protein-protein interactions visualized by bimolecular fluorescence complementation in tobacco protoplasts and leaves. J Vis Exp **85:** 51327

Senthil-Kumar M, Mysore KS (2013) Nonhost resistance against bacterial pathogens: retrospectives and prospects. Annu Rev Phytopathol **51:** 407–427

Shamloul M, Trusa J, Mett V, Yusibov V (2014) Optimization and utilization of *Agrobacterium*-mediated transient protein production in *Nicotiana*. J Vis Exp **86:** 51204

Stein M, Dittgen J, Sánchez-Rodríguez C, Hou BH, Molina A, Schulze-Lefert P, Lipka V, Somerville S (2006) *Arabidopsis* PEN3/PDR8, an ATP binding cassette transporter, contributes to nonhost resistance to inappropriate pathogens that enter by direct penetration. Plant Cell **18:** 731–746

Sumit R, Sahu BB, Xu M, Sandhu D, Bhattacharyya MK (2012) Arabidopsis nonhost resistance gene *PSS1* confers immunity against an oomycete and a fungal pathogen but not a bacterial pathogen that cause diseases in soybean. BMC Plant Biol **12:** 87

Swaminathan S, Abeysekara NS, Liu M, Cianzio SR, Bhattacharyya MK (2016) Quantitative trait loci underlying host responses of soybean to *Fusarium virguliforme* toxins that cause foliar sudden death syndrome. Theor Appl Genet **129:** 495–506

Tao TY, Ouellet T, Dadej K, Miller SS, Johnson DA, Singh J (2006) Characterization of a novel glycine-rich protein from the cell wall of maize silk tissues. Plant Cell Rep **25:** 848–858

Tavares LS, Rettore JV, Freitas RM, Porto WF, Duque AP, Singulani JdeL, Silva ON, Detoni MdeL, Vasconcelos EG, Dias SC, et al (2012) Antimicrobial activity of recombinant Pg-AMP1, a glycine-rich peptide from guava seeds. Peptides **37:** 294–300

Teh OK, Hofius D (2014) Membrane trafficking and autophagy in pathogen-triggered cell death and immunity. J Exp Bot **65:** 1297–1312

Ueki S, Citovsky V (2002) The systemic movement of a tobamovirus is inhibited by a cadmium-ion-induced glycine-rich protein. Nat Cell Biol **4:** 478–486

Ueki S, Citovsky V (2005) Identification of an interactor of cadmium ion-induced glycine-rich protein involved in regulation of callose levels in plant vasculature. Proc Natl Acad Sci USA **102:** 12089–12094

Wang B, Swaminathan S, Bhattacharyya MK (2015) Identification of *Fusarium virguliforme* FvTox1-interacting synthetic peptides for enhancing foliar sudden death syndrome resistance in soybean. PLoS ONE **10:** e0145156

Weigel D, Glazebrook J (2006) Transformation of Agrobacterium using the freeze-thaw method. CSH Protoc **2006:** 1031–1036

Winter D, Vinegar B, Nahal H, Ammar R, Wilson GV, Provart NJ (2007) An "Electronic Fluorescent Pictograph" browser for exploring and analyzing large-scale biological data sets. PLoS ONE **2:** e718

Woloshen V, Huang S, Li X (2011) RNA-binding proteins in plant immunity. J Pathogens **2011:** 278697

Yoshimoto K, Hanaoka H, Sato S, Kato T, Tabata S, Noda T, Ohsumi Y (2004) Processing of ATG8s, ubiquitin-like proteins, and their deconjugation by ATG4s are essential for plant autophagy. Plant Cell **16:** 2967–2983

Zhang Y (2008) I-TASSER server for protein 3D structure prediction. BMC Bioinformatics **9:** 40

Zhang Y, Skolnick J (2005) TM-align: a protein structure alignment algorithm based on the TM-score. Nucleic Acids Res **33:** 2302–2309